Vaccination strategies to control Ebola epidemics in the context of variable household inaccessibility levels

G. Chowell[*1], A. Tariq[1], M. Kiskowski[2]

[1]Department of Population Health Sciences, School of Public Health, Georgia State University, 30303, Atlanta, GA, USA

[2]Department of Mathematics and Statistics, University South Alabama, 36688, Mobile, AL, USA

[*]Corresponding author

Abstract

Despite a very effective vaccine, active conflict and community distrust during the ongoing DRC Ebola epidemic are undermining control efforts, including a ring vaccination strategy that require the prompt immunization of close contacts of infected individuals. However, 20% or more of close contacts cannot be reached or refused vaccination [1], and it is predicted that the ring vaccination strategy would not be effective with such a high level of inaccessibility. In May 2019, the DRC expanded their control efforts to include a community vaccine strategy. To assess the impact of vaccination strategies for controlling Ebola epidemics in the context of variable levels of community resistance, we employed an individual-level stochastic transmission model that incorporates three sources of heterogeneity namely a proportion of the population is inaccessible for effective contact tracing and vaccination efforts due to lack of confidence in interventions or geographic inaccessibility, two levels of population mixing resembling household and community transmission, and spatial dependence on transmission rates. Our results indicate that a ring vaccination strategy would not be effective for containing the epidemic if levels of inaccessibility are too high and estimate the impact of a supplemental community vaccination strategy. Our key results are that as levels of inaccessibility increase, there is a qualitative change in the effectiveness of the vaccination strategy. For lower levels of inaccessibility, the probability of epidemic containment increases over time, even if probabilities are lower than they would be otherwise. For higher levels of inaccessibility, vaccination strategies are not expected to contain the epidemic even though they help lower incidence levels, which saves lives, makes the epidemic easier to contain and reduces spread to other communities. This qualitative change occurs for both types of vaccination strategies: ring vaccination is effective for containing an outbreak until the levels of inaccessibility exceeds approximately 30%, a combined ring and community vaccination strategy is effective until the levels of inaccessibility exceeds approximately 50%. More broadly, our results underscore the need to enhance community engagement to public health interventions in order to enhance the effectiveness of control interventions to ensure outbreak containment.

Keywords: Mathematical modeling, individual-based model, Ebola, vaccination strategies, ring vaccination, community vaccination, community accessibility, community resistance, epidemic containment, endemic state, epidemic wave.

Introduction

A key lesson from past Ebola outbreaks indicates that their containment hinges on educating local communities in order to fight misinformation relating to the transmission of the virus in the population and the role of control interventions as well as community mistrust of the response teams [2, 3]. These educational activities are critical for the successful deployment of contact tracing and surveillance efforts, treatment and management of Ebola cases, and promoting behaviors that mitigate transmission rates [4]. However, the ongoing Ebola outbreak in the Democratic Republic of Congo (DRC), which has been active in the region for about 10 months (August 2018 to May 2019), has become the most complex Ebola epidemic to date, threatening to spread to neighboring countries. In particular, this unprecedented epidemic is unfolding in a climate of community distrust in the interventions [5, 6] in an active conflict zone [7], where over one hundred attacks have deliberately targeted healthcare workers and treatment centers involved in the Ebola response efforts, allowing sustained transmission in the region. Consequently, the DRC Ebola epidemic, which has accumulated 1866 cases including 1241 deaths as of May 21st, 2019 [8], is far from containment, with a surge in Ebola incidence during the last few weeks, coinciding with an increasing trend in the number of violent attacks on health centers and health teams fighting the epidemic in the region [9].

Although control efforts now employ a highly effective emergency vaccine, the ongoing Ebola epidemic in the DRC is the first to occur in an active conflict zone.

Deliberate violent attacks and threats to health workers on a scale not seen in previous Ebola outbreaks are directly undermining active control efforts in the region [7]. A ring vaccination strategy [10, 11] that was highly effective in the capital [12] was introduced rapidly on August 8th, 2018 within 8 days of the outbreak declaration in the provinces of North Kivu and Ituri [13]. However, it has been challenging to implement an effective ring vaccination strategy in a climate of violence targeting healthcare workers and decreasing accessibility to a mobile, fractionated population as it relies on the identification of contacts and contacts of contacts [14]. This issue is compounded by a large fraction of Ebola cases unconnected to known chains of transmission [15]. In order to boost the impact of the vaccine in a challenging transmission setting with a large fraction of hidden or underground transmission, the vaccination strategy is now incorporating community-level vaccination. The community-level vaccination strategy will immunize members of communities even if they are not known contacts of Ebola cases using a lower vaccine dose, which will take longer to elicit protective antibody levels in vaccinated individuals [16, 17].

Here we sought to evaluate the impact of Ebola control efforts including vaccination campaigns by extending an individual-based model with household-community mixing [18, 19], which has been previously used to analyze the effects of different levels of population mixing on Ebola transmission dynamics. This model has been able to fit the growth patterns of the 2014-15 Western Africa Ebola epidemic by calibrating the extent of community mixing [18]. This structured transmission model predicts outbreaks that propagate through the population as spatial waves with a endemic

state [19] and has been useful to gain insight on the level of control that would be required to contain Ebola epidemics [19].

Assessing the effect of targeted vaccination efforts requires mathematical models that capture the contact structure of the community network [20-24]. In our paper, we aimed to investigate the effect of ring [20, 22, 25-27] and community vaccination strategies on outbreak control. For this purpose, our baseline stochastic model, which has been calibrated using data for the Western African Ebola epidemic [18, 19], was adapted to incorporate key features of the Ebola epidemic in the DRC. Specifically, we evaluate the effectiveness of control strategies in the context of a fraction of the population that is inaccessible to vaccination teams, tied to the success of contact tracing and vaccination efforts. Our baseline network transmission model also adapts for the ring vaccination strategy by integrating heterogeneity in community transmission rates that scale with the distance between an infectious individual and each member of that individual's community. Ring and community vaccination strategies are compared by accounting for the different spatial scales for the radius of contacts that are vaccinated and the different time scales for the vaccination and immunization of their susceptible and exposed contacts.

Methods

Household-Community Model for Ebola Spread and Two Types of Vaccination with Accessible and Inaccessible Households

We previously described our model for disease spread [18, 19] and vaccination [28] in a contact network with household-community structure. A new component of our model is that we add a second type of household that is inaccessible to vaccination teams. These households may not participate for a variety of reasons including Ebola cases that are not identified, lack of confidence in the vaccination program and geographic inaccessibility. The inaccessible households do not participate in vaccination and do not provide contacts lists. We also modify the model to include two vaccine types. A larger vaccine dose is used for ring vaccination with faster immunization occurring 10 days later, and a smaller vaccine dose is used for community vaccination with immunization occurring 28 days later. This corresponds to the dosing and predicted timing of the ring and community vaccination regimens of 0.5 ml and 0.2 ml doses, respectively, recently described for the DRC Ebola epidemic [14, 16].

Disease and Vaccination States

The progression of Ebola disease, vaccination and immunization are modeled with seven epidemiological states (S, E, I, R, Svr, Svc, M); four SEIR states for Ebola disease progression (susceptible S, exposed E, infectious I and refractory R) and three states for vaccination progression (two susceptible but vaccinated states S_{VR} and S_{VC} and an immune state M) (see Figure 1). The states Svc and Svr are assigned to individuals vaccinated by community or ring vaccination. Individuals with these states remain susceptible to Ebola exposure. After a delay of 10 days for Svr or 28 days for Svc, the individuals become immune transitioning to state M.

Individuals in three epidemiological states (S, Svc and Svr) are at risk of contracting Ebola from infectious individuals (I), transitioning to the latent period (exposed state E). Transition rates from any of these three susceptible states to the exposed state depend on the contact network and increase with the number of infectious contacts. In our model, individuals in the exposed state E (latency) are no longer available for effective vaccination and immunization. Thus, if an individual is indicated to be vaccinated by either the ring or community vaccination programs, they may be approached by a vaccination team and given the vaccine since their exposure status is unknown, but once in the Exposed class, they may not change states to the susceptible states Svc or Svr. Once exposed, nodes transition from the exposed (E) to infectious class (I) with probability $\frac{1}{\gamma}$ per day where $\gamma = 5.3$ days is the average incubation period [29-32] and once infectious, nodes transition from the infectious (I) to refractory class (R) with probability $\frac{1}{\lambda}$ per day, where $\lambda = 5.6$ days is the average infectious period [29-32]. Parameter definitions and values used in simulations and their sources are given in Table 1.

Contact Network with Household and Community Structure

As in refs. [18, 19, 28], we model the spread of Ebola on a contact network that consists of households of size H that are organized in communities of size C households. Households are arranged one-dimensionally within an LxH array where L is the number of households in the contact network N. Households are indexed $\{h_i, h_{i+1}, \dots\}$ and a network distance η between two households h_i and h_j is defined as

$\eta=|i-j|$. The i_{th} community is centered at the ith household and includes all of the households within a radius Rc of the i_{th} household (for a community containing C households, the community radius is Rc=(C-1)/2. This contact network is highly mutually connected, the extent of overlap between the i_{th} and j_{th} communities depend on the network distance of the i_{th} and j_{th} households in that communities of nearby households overlap and share most households. Due to this high mutual connectivity and linear arrangement of the contact network, saturation effects build up quickly and disease progresses spatially as 1-dimensional wave through the lattice network. The size of the contact network and the size of the simulated population is unlimited since the lattice size LxH is dynamic and extends as needed as the disease and immunity extends through the population.

In this version of the model, each household is designated as accessible or inaccessible (see Figure 2). This assignment is random and once a household is labeled, this assignment does not change. During the initial construction of the contact network, and as the array is dynamically extended, households are labeled inaccessible with probability β, otherwise the household is accessible. Here we compare results as a function of the fraction of inaccessible households between 0 and 40% (30% non-participating individuals were estimated for a vaccination program that will be expanded to younger age groups in [33]; the program was approved for expansion to younger age groups in the first half of 2019 [34]).

Distance Dependent Transmission Rates

At the onset of an epidemic, before the accumulation of saturation effects so that all nodes of the network are susceptible except for a single infectious case, the household reproductive number $R0_H$ is the average number of secondary infections within the household of the infected individual and the community reproductive number $R0_C$ is the average number of secondary infections within the community. As in ref. [19], we set $R0_H$ =2.0 infections within the household and $R0_C$ =0.7 infections within the community based on R_0 within household and communities in historical Ebola epidemics [4, 18, 29, 35].

<u>Transmission rates for homogenous network transmission</u>: In the simplest case of homogeneous transmission rates, all members of a household have an equal probability of infection from an infectious contact, and all members of a community have an equal probability of infection from an infectious contact. Transmission rates within the household and within the community are normalized so that the reproductive number of household and community infections are $R0_H$ and $R0_C$, respectively. Since, there are H-1 household contacts within the household of a single infectious individual, and $(CH - H)$ community contacts within the community of a single infectious individual, for a fixed infectious period λ, household and community transmission rates for each infectious-susceptible contact are given by:

$$t_H := \frac{R_{0H}}{\lambda\,(H-1)},\ t_C := \frac{R_{0C}}{\lambda\,(C \cdot H - H)}.$$

However, as described in refs. [36, 37], for exponentially distributed infectious periods λ, household and community transmission rates for each infectious-susceptible contact would be:

$$t_H := \frac{R_{0H}}{\lambda\,(H-1-R_{0H})}\,,\; t_C := \frac{R_{0C}}{\lambda\,(C\cdot H-H-R_{0C})}.$$

Since there are $(CH - H)$ community contacts, the total rate of community transmission in the network (for a single infectious individual with all other nodes susceptible) would be $(CH - H) \cdot t_C$.

<u>Transmission rates for distance-dependent network transmission</u>: In ref. [28], we introduced distance-dependent transmission so that within the community, the transmission rate decreases with the distance between the infectious and susceptible individuals. For any distance function f(η), transmission rates on the network may be scaled to yield a given set of reproductive numbers $R0_H$ and $R0_C$. This is accomplished by assigning values α·f(η) to each community contact and choosing α so that the sum of transmission rates along every edge is equal to $(CH - H) \cdot t_C$. Initial transmission rates when all contacts are susceptible are $R0_H$ infections per household and $R0_C$ infections within the community. As the number of exposed nodes accumulate, actual transmission rates decrease due to saturation effects that depend on the radial profile of the transmission function. Thus, spread of an infection depends on this transmission profile, as well as the household and community reproductive numbers and the network structure itself.

Here we consider relatively simple distance-dependent transmission profiles in which transmission rates decrease exponentially with distance using the function $f(\eta) = e^{k\eta}$n that we used in ref. [28] or inversely with distance using the function $g(\eta) = \frac{1}{\eta^k}$ (the intuitive “gravity model” from transportation theory [38, 39] , for the case of

households of equal size as we have here). The normalized transmission profiles are shown in Figure 3. Other transmission functions that depend on distance may be more complex exponential forms (e.g. beta-pert distributed as in ref. [40]).

Community and Ring Vaccination

We model two types of vaccination. Ring vaccination is the vaccination of household members and other close contacts defined as members of the community within a radius Rv. Community vaccination is the vaccination of members of the entire community. Both types of vaccination occur on a daily basis, for flexible start and end times.

Ring vaccination: On the day D that an infectious individual within an accessible household becomes infectious, the infectious individual provides a list of their close contacts (household members and members of the community within radius R_{VR}). Ring vaccination occurs after delay of τ days so that vaccination occurs on D+τ. A delay of $\tau = 2$ days was chosen as in ref. [33]. Ring vaccination begins on a number of days Vstart after a simulation begins with one infectious case. If ring vaccination has begun by day D, then members added to contact lists on day D are vaccinated on day D+τ (their state changes from S to S_{VR}) if they are susceptible, not yet vaccinated, and located within an accessible household. The radius R_{VR}=5 households was chosen based on the household size of H=5 to include 55 individuals. This was based on the identification of 50 contacts per infectious case during the Guinea ring vaccination trial [10].

Community vaccination: If community vaccination is occurring on a given day D, all community contacts of infectious individuals will be vaccinated with rate r_{VC} if they are susceptible, not yet vaccinated, and located within accessible households. Vaccination rate of 5% and 10% were studied, corresponding to a program in which most accessible members of the community are vaccinated in 20 or 10 days.

We do not model exponentially distributed immunity rates. Rather, immunization occurs for individuals with state S_{VR} after 10 days and for individuals with state Svc after 28 days. It is possible that an individual is vaccinated with community vaccination and then discovers they are a close contact of an infectious individual, where ring vaccination is indicated. Because of this, a spike may occur when community vaccination is initiated, due to the comparable delay of protection for these individuals. We optimistically model that the individual can be ring vaccinated as well, either with a supplemental or additional vaccine dose, will be immunized by whichever vaccine would mature first.

Simulation Description, and Fitting of the Community Size C

For a typical simulation, the simulation is initiated on Day 1 with a single infectious individual centered within a single community. With each newly exposed individual, the contact network is dynamically extended to include the community of every exposed individual. As the simulation is run, disease and vaccination states accumulate in the network and the algorithm keeps track of the state of each node for each day. Disease and/or vaccination states progress as a linear wave through the contact network. Outbreaks die out spontaneously when all members of the contact network are susceptible, refractory or immune.

The average growth of an epidemic per day is computed as the average number of cases versus day for 500 simulations. The average number of cases for the nth day is averaged only for the number of simulations that have not yet extinguished by day n. While $R0_H$ and $R0_C$ are parameters that we consider intrinsic to the virology of Ebola, the community size C is an abstract quantity that is meant to capture the net effect of community interactions that describe the accumulation of saturation effects. In ref. [18], we found that different community sizes would result in different steady state levels for the number of cases per day, so that regions with a larger growth rate have a larger community size. The community size C must also be calibrated for each transmission profile. We choose the community size for each transmission profile by assuming that an outbreak in North Kivu would be similar in size to the 2014-15 Ebola outbreak in Liberia, which was not affected by vaccination.

Model Limitations

We have made several simplifying assumptions. We assume that the day an individual becomes infectious is also the day when an individual becomes symptomatic. If the individual belongs to an accessible household, they will be identified as an Ebola case on that day. We assumed that already exposed individuals could not benefit from vaccination before becoming infectious. However, there is evidence that vaccination after exposure can reduce Ebola symptoms and would likely decrease transmission of the infectious individual and for this reason in ref. [33] researchers estimated a slighter lower time to immunization of 7 rather than 10 days for the 0.5 ml ring vaccine dose. We assumed that the vaccines are 100% effective, and that they are effective after a

307 fixed rather than random time interval. Evidence indicates that the vaccine efficacy is
308 close to 100% [10]. By assuming a 100% vaccine effectiveness, we assume that the
309 effects of non-participation in vaccination or unvaccinated community contacts are a
310 much larger effect than a small percentage of vaccine failures.
311 There are many unknowns regarding the parametrization of the household community
312 structure. We chose a community size that would match the incidence observed in
313 Liberia during the West African Ebola epidemic, in the absence of vaccination, but this
314 community size depends on the transmission profile as a function of distance that is
315 unknown. The community size and the transmission profile together should be
316 interpreted as a summary of complex network interactions that result in an observed
317 incidence, and are not constrained by the currently available data. We model a
318 random distribution of inaccessible households, whereas they may be clustered (also
319 as in ref. [33]). Finally, we simulate epidemics in the context of community
320 transmission in the absence of long-range links, so we cannot capture the effects of
321 missed contacts that seed outbreaks in new locations (and the initial faster growth of
322 those outbreaks in naïve communities).
323
324
325

Table 1. Parameter values used in simulations**.** Description of each model parameter, the value or range that is used, and the reference source for the value that is used if applicable.

Parameter	Description	Parameter Value (Range)	Source
H	Household Size	5	[18, 19] and [28]
C	Community Size	201	–
B	Fraction of households that are inaccessible.	0.0-0.6	–
R_{0H}	Household reproductive number	2.0	[19]
R_{0C}	Community reproductive number	0.7	[19]
Γ	Average incubation period	5.3 days	[4, 32]
Λ	Average infectious period	5.6 days	[4, 30]
R_{VR}	Radius of ring vaccination (number of households)	5	[10]
r_{VC}	Rate of community vaccination	0.05, 0.2	–
τ	Days to vaccinate an individual with the ring vaccination program	2	[33]
d_{VR}	Days till immunity for 0.2 ml vaccine	10	[14, 16]
d_{VC}	Days till immunity for 0.2 ml vaccine	28	[14, 16]
$Vstart_r$	Day of start of the ring vaccination campaign	0-9 months	
$Vstart_c$	Day of start of the community vaccination campaign	0-9 months	

Results

Incidence and extinction with no vaccine interventions

In the absence of vaccination, our calibrated model predicts that case incidence grows during the first 10 serial intervals and then surviving epidemic realizations reach a stable case incidence around 41-46 cases per day (Figure 4). A significant fraction of epidemic realizations dies out; about 19-30% of the epidemic realizations spontaneously extinguish early on, within the first 30 days of the simulation (Figure 4). Once epidemic realizations have persisted several serial intervals, they become robust to extinction with a very low extinction rate.

Incidence and extinction with ring vaccination

Our results indicate that the impact of a ring vaccination strategy heavily depends on the fraction of inaccessible households in the population. In the best-case scenario when all households are accessible ($\beta=0$), the probability of epidemic control increases linearly over time with a ring vaccination strategy that starts 30 days after epidemic onset (Figure 5). Since epidemic realizations are likely to end spontaneously within the first 30 days, the effect of ring vaccination applied after 30 days shows the effect of ring vaccination on the fraction of remaining epidemics that would otherwise likely persist. Data from the curves in Figure 5 showing this increase in the probability of epidemic control over time are summarized in Table 2. Over 6, 12, and 18 months, the probability of epidemic control for a fully accessible population is 26-34%, 41-50%, and

62-70%, respectively. Moreover, this probability of epidemic control does not change significantly when the ring vaccination program starts only 7 days after epidemic onset (data not shown). At a 10% level of household inaccessibility, the probability of epidemic control decreases relative to the case of full accessibility (curves in Figure 5, Panel A or the data summary in Table 2) but the probability that the epidemic is controlled still accumulates steadily over time. At 30-50% levels of household inaccessibility, the pattern is qualitatively different. The probability of epidemic control no longer increases with the application of ring vaccination and rapidly saturates around 19-29%, just as it would without the application of ring vaccination. However, the trajectory of outbreak incidence conditional on non-extinction stabilizes around 12-22 cases per day, which is markedly lower than the case of no ring vaccination (Figure 5).

These results for vaccination applied at 30 days show that for high fractions of inaccessible households, ring vaccination has little effect on ending an epidemic but substantially decreases the size of the epidemic. This pattern is robust to the timing of start of the ring vaccination program: when ring vaccination is applied to an established epidemic wave after 9 months, there is no effect on the lifetime of the epidemic but the steady state incidence decreases (Figure 6). Ring vaccination applied after 9 months decreases steady state incidence to the same values as ring vaccination applied earlier, after 30 days (Figure 5).

Table 2. Comparison of the probability of epidemic control for ring vaccination starting 30 days after epidemic onset versus no vaccination, for different fractions of inaccessible households. Intervals show the 95% confidence interval. Since this interval varies slightly from one set of epidemic realizations to another, intervals that are statistically comparable to the case of non-vaccination are simplified in their description as "<31%".

	Probability of extinction: in the absence of vaccination	After ring vaccination strategy applied for 6 months	After ring vaccination strategy applied for 12 months	After ring vaccination strategy applied for 18 months
0% inaccessible households	19-30%	26-34%	41-50%	62-70%
10% inaccessible households	19-30%	22-30%	30-38%	41-50%
20% inaccessible households	19-30%	19-26%	21-29%	24-31%
30% inaccessible households	19-30%	<31%	<31%	<31%
40% inaccessible households	19-30%	<31%	<31%	<31%
50% inaccessible households	19-30%	<31%	<31%	<31%

Community vaccination that supplements a ring vaccination strategy can significantly increase the probability of epidemic control.

For the scenario resembling the DRC Ebola epidemic where a ring vaccination strategy starts one week after epidemic onset and is subsequently supplemented with community vaccination 9 months later, we found that the community vaccination strategy substantially increases the probability of extinction, after a delay, and can substantially decrease the endemic state (Figure 7). However, the probability of achieving epidemic control again appears to not be improved when the fraction of inaccessible household is too high (e.g., 50% inaccessible; Figure 7). Figure 8 illustrates the effects of the community vaccination rates on case incidence and the probability of epidemic control. The supplemental effect of community vaccination on the probability of epidemic extinction for populations with different levels of inaccessible households ranging from 0 to 50% are summarized in Figure 9. After 3 years of disease transmission, our model-based results indicate that the probability of epidemic control is at 88-93% for a 30% level of household inaccessibility and 52-61% for a 40% household inaccessibility level.

Discussion

In this paper we have employed an individual-level stochastic transmission model to evaluate ring and community vaccination strategies for containing Ebola epidemics in the context of varying levels of community accessibility to public health interventions. Our individual-based model, which was calibrated based on the transmission dynamics of the 2014-15 Western African Ebola epidemic in the absence of vaccination, incorporates three sources of heterogeneity including a proportion of the population

that is inaccessible for effective contact tracing and vaccination efforts due to lack of confidence in interventions or geographic inaccessibility, two levels of population mixing resembling household and community transmission, and spatial dependence on transmission rates. Our findings indicate that ring vaccination, which targets a radius of contacts for each infectious individual, is an effective intervention to contain Ebola epidemics with relatively low levels of household inaccessibility (<30%). At higher levels of household inaccessibility, ring vaccination could be useful for reducing the disease endemicity level, but it is no longer an effective intervention to ensure outbreak containment in the absence of any other interventions. We also found that community vaccination strategies that supplement a ring vaccination strategy can speed up and enhance the probability of epidemic containment but only for moderate levels of household inaccessibility (e.g., <50%). For instance, our results for the scenario motivated by the DRC Ebola epidemic predict a probability of epidemic containment at about 90% after 3 years of disease transmission for a 30% household inaccessibility level. More generally, our results highlight the critical need to enhance community engagement to public health interventions while offering a safe and secure environment to the population in order to increase the effectiveness of control interventions to ensure outbreak containment.

Active local conflict and community mistrust of the government and public health authorities hamper containment of epidemics driven by person-to-person transmission [5]. In this context, it is particularly important that health communication and community education efforts are coordinated and implemented in collaboration with the affected communities [2]. Findings from a recent survey in DRC indicate that about

25-32% of the population is skeptical about the reality of the Ebola epidemic and/or distrust local public health authorities [41]. Importantly, there is some evidence that Ebola outbreak in DRC is being perceived in the region as a political tool against certain groups while some other groups benefit politically and financially from the ongoing epidemic [42] . This underscores the need to ensure that the Ebola response is entirely isolated from political biases to avoid exacerbating resource inequality and distrust in the institutional authorities. Indeed, there is significant evidence that supports the implementation of integrative communal approaches to prevent rumor spreading, distrust and fear about Ebola in the communities and help improve epidemiological surveillance and enhance the adoption of Ebola preventive measures [2, 43-45].

In contrast to the simple SIR compartmental transmission models based on homogenous mixing assumptions that support bell-shaped epidemic trajectories [46, 47] [48, 49], our spatially structured stochastic model employed in this study has been able to successfully capture stationary disease waves where the virus moves through the host population over time. This transmission pattern is qualitatively similar to those of the ongoing Ebola epidemic in DRC [8, 50]. In particular, they achieve relatively steady incidence levels as Ebola spreads from one community to another, and the total incidence can be interpreted as the super-positioning of the cases from a discrete number of communities involved rather than explosive exponential growth. However, our model does not predict sporadic increases in case incidence, as in the most recent surge in case incidence [51], which is not surprising as our model does not incorporate time-dependent changes in the effectiveness of control interventions tied to violent attacks to healthcare workers and public health infrastructure. From an

epidemic modeling perspective, our results underscore the need to capture an appropriate spatial structure in models of disease transmission [18, 22-24, 52, 53]. Such considerations may be more important for infectious diseases that are transmitted via close contact such as Ebola and HIV.

In summary, we found that the role of vaccination strategies in containing Ebola epidemics significantly depends on the level of community inaccessibility using an individual-level stochastic transmission model that successfully captures stationary disease waves that are qualitatively similar to those of the ongoing Ebola epidemic in DRC. For lower levels of inaccessibility, the probability of containment increases over time. For higher levels, vaccination strategies alone are not expected to contain the epidemic, but they help reduce incidence levels, which saves lives, makes the epidemic easier to contain and reduces spread to other communities. This qualitative change occurs for both types of vaccination strategies: ring vaccination is effective for containing an outbreak until the level of inaccessibility exceeds approximately 30%, a combined ring and community vaccination strategy is effective until the level of inaccessibility exceeds approximately 50%. In order to enhance the effectiveness of control interventions, it is crucial to ensure community engagement to public health interventions.

Conflict of interest

The authors declare no conflicts of interest.

References

1. Cohen, J., *Ebola outbreak continues despite powerful vaccine. Available from: https://science.sciencemag.org/content/364/6437/223*. Science, 2019.
2. Marais, F., et al., *A community-engaged infection prevention and control approach to Ebola.* Health Promot Int, 2016. **31**(2): p. 440-9.
3. Nyenswah, T.G., et al., *Ebola and Its Control in Liberia, 2014-2015.* Emerg Infect Dis, 2016. **22**(2): p. 169-77.
4. Chowell, G. and H. Nishiura, *Transmission dynamics and control of Ebola virus disease (EVD): a review.* BMC Med, 2014. **12**(1): p. 196.
5. Vinck, P., et al., *Institutional trust and misinformation in the response to the 2018-19 Ebola outbreak in North Kivu, DR Congo: a population-based survey.* Lancet Infect Dis, 2019. **19**(5): p. 529-536.
6. Nguyen, V.K., *An Epidemic of Suspicion - Ebola and Violence in the DRC.* N Engl J Med, 2019. **380**(14): p. 1298-1299.
7. Claude, K.M., J. Underschultz, and M.T. Hawkes, *Ebola virus epidemic in war-torn eastern DR Congo.* Lancet, 2018. **392**(10156): p. 1399-1401.
8. *Ebola virus disease – Democratic Republic of the Congo. Disease outbreak news: Update for 23 April 2019. Available from: https://www.who.int/csr/don/23-may-2019-ebola-drc/en/ (accessed on 24 May 2019).*
9. *Kivu Security Tracker. Available from: https://kivusecurity.org/map#.*
10. Henao-Restrepo, A.M., et al., *Efficacy and effectiveness of an rVSV-vectored vaccine expressing Ebola surface glycoprotein: interim results from the Guinea ring vaccination cluster-randomised trial.* Lancet, 2015. **386**(9996): p. 857-66.
11. Merler, S., et al., *Containing Ebola at the Source with Ring Vaccination.* PLoS Negl Trop Dis, 2016. **10**(11): p. e0005093.
12. Wells, C.R., et al., *Ebola vaccination in the Democratic Republic of the Congo.* Proc Natl Acad Sci U S A, 2019. **116**(20): p. 10178-10183.
13. *WHO. Ebola virus disease – Democratic Republic of the Congo. 2018 [cited 2018 August 19]; Available from: https://www.who.int/csr/don/17-august-2018-ebola-drc/en/.*
14. *The report of the SAGE April 2019 will be published in the WHO Weekly Epidemiological Record (www.who.int/wer/en/) on 30 May 2019.*

15. *Maxmen, A. Ebola detectives race to identify hidden sources of infection as outbreak spreads. Available from: https://www.nature.com/articles/d41586-018-07618-0 (accessed on 23 May 2019).*
16. Cohen, J., *DRC expands Ebola vaccine campaign as cases mount rapidly.* Science.
17. *World Health Organization. Interim Recommendations on Vaccination against Ebola Virus Disease (EVD). Available from: https://www.who.int/immunization/policy/position_papers/interim_ebola_recommendations_may_2019.pdf?ua=1 (accessed on 20 May 2019).*
18. Kiskowski, M., *Three-Scale Network Model for the Early Growth Dynamics of 2014 West Africa Ebola Epidemic.* . PLOS Currents Outbreaks, 2014. **doi: 10.1371/currents.outbreaks.b4690859d91684da963dc40e00f3da81.**
19. Kiskowski, M. and G. Chowell, *Modeling household and community transmission of Ebola virus disease: epidemic growth, spatial dynamics and insights for epidemic control.* Virulence, 2015. **7**(2): p. 63-73.
20. Tildesley, M.J., et al., *Optimal reactive vaccination strategies for a foot-and-mouth outbreak in the UK.* Nature, 2006. **440**(7080): p. 83-6.
21. Ferguson, N.M., C.A. Donnelly, and R.M. Anderson, *The foot-and-mouth epidemic in Great Britain: pattern of spread and impact of interventions.* Science, 2001. **292**(5519): p. 1155-60.
22. Browne, C., H. Gulbudak, and G. Webb, *Modeling contact tracing in outbreaks with application to Ebola.* J Theor Biol, 2015. **384**: p. 33-49.
23. Lau, M.S.Y., et al., *A mechanistic spatio-temporal framework for modelling individual-to-individual transmission-With an application to the 2014-2015 West Africa Ebola outbreak.* PLoS Comput Biol, 2017. **13**(10): p. e1005798.
24. Yang, W., et al., *Transmission network of the 2014-2015 Ebola epidemic in Sierra Leone.* J R Soc Interface, 2015. **12**(112).
25. Greenhalgh, D., *Optimal control of an epidemic by ring vaccination.* Communications in Statistics. Stochastic Models, 1986. **2**(3): p. 339--363.
26. Muller, J., B. Schonfisch, and M. Kirkilionis, *Ring vaccination.* J Math Biol, 2000. **41**(2): p. 143-71.
27. Kretzschmar, M., et al., *Ring vaccination and smallpox control.* Emerg Infect Dis, 2004. **10**(5): p. 832-41.
28. Chowell, G. and M. Kiskowski, *Modeling ring-vaccination strategies to control Ebola virus disease epidemics*, in *Mathematical modelling for emerging and*

reemerging infectious diseases, G. Chowell and J.M. Hyman, Editors. 2016, Springer.

29. Chowell, G., et al., *The basic reproductive number of Ebola and the effects of public health measures: the cases of Congo and Uganda.* J Theor Biol, 2004. **229**(1): p. 119-26.

30. Legrand, J., et al., *Understanding the dynamics of Ebola epidemics.* Epidemiol Infect, 2007. **135**(4): p. 610-21.

31. Lekone, P.E. and B.F. Finkenstadt, *Statistical inference in a stochastic epidemic SEIR model with control intervention: Ebola as a case study.* Biometrics, 2006. **62**(4): p. 1170-7.

32. Eichner, M., S.F. Dowell, and N. Firese, *Incubation period of ebola hemorrhagic virus subtype zaire.* Osong Public Health Res Perspect, 2011. **2**(1): p. 3-7.

33. Kucharski, A.J., et al., *Effectiveness of Ring Vaccination as Control Strategy for Ebola Virus Disease.* Emerg Infect Dis, 2016. **22**(1): p. 105-8.

34. *ReliefWeb Report. UNICEF DR Congo Ebola Situation Report North Kivu and Ituri - 03 February 2019. Available from: https://reliefweb.int/report/democratic-republic-congo/unicef-dr-congo-ebola-situation-report-north-kivu-and-ituri-03*.

35. Althaus, C.L., *Estimating the reproduction number of Zaire ebolavirus (EBOV) during the 2014 outbreak in West Africa.* PLOS Currents Outbreaks. Edition 1. doi: 10.1371/currents.outbreaks.91afb5e0f279e7f29e7056095255b288., 2014.

36. Lloyd AL, V.S., Cintrón-Arias A., *Infection dynamics on small-world networks.* Contemp Math. , 2006. **410**: p. 209.

37. Keeling, M.J. and B.T. Grenfell, *Individual-based perspectives on R(0).* J Theor Biol, 2000. **203**(1): p. 51-61.

38. Xia, Y.C., O.N. Bjørnstad, and B.T. Grenfell, *Measles metapopulation dynamics: a gravity model for epidemiological coupling and dynamics.* Am Nat 2004. **164**: p. 267-81.

39. Viboud, C., et al., *Synchrony, waves, and spatial hierarchies in the spread of influenza.* Science, 2006. **312**(5772): p. 447-51.

40. Durr, S. and M.P. Ward, *Development of a Novel Rabies Simulation Model for Application in a Non-endemic Environment.* PLoS Negl Trop Dis, 2015. **9**(6): p. e0003876.

41. Schnirring, L. *As Ebola rages in DRC, survey highlights wide mistrust, in CIDRAP News.Available from: http://www.cidrap.umn.edu/news-*

perspective/2019/03/ebola-rages-drc-survey-highlights-wide-mistrust (accessed on 05 May 2019).

42. Aizenman, N. *Why The Ebola Outbreak In The Democratic Republic Of Congo Keeps Getting Worse. NPR News. Available from: https://www.npr.org/2019/05/23/725789837/why-the-ebola-outbreak-in-the-democratic-republic-of-congo-keeps-getting-worse (accessed on 23 May 2019).*
43. Tambo, E., E.C. Ugwu, and J.Y. Ngogang, *Need of surveillance response systems to combat Ebola outbreaks and other emerging infectious diseases in African countries.* Infect Dis Poverty, 2014. **3**: p. 29.
44. Thiam, S., et al., *Challenges in controlling the Ebola outbreak in two prefectures in Guinea: why did communities continue to resist?* Pan Afr Med J, 2015. **22 Suppl 1**: p. 22.
45. Buseh, A.G., et al., *The Ebola epidemic in West Africa: challenges, opportunities, and policy priority areas.* Nurs Outlook, 2015. **63**(1): p. 30-40.
46. Anderson, R.M. and R.M. May, *Infectious diseases of humans*. 1991, Oxford: Oxford University Press.
47. Hethcote, H.W., *The mathematics of infectious diseases.* SIAM review, 2000. **42**(4): p. 599-653.
48. Brauer, F., *Some simple epidemic models.* Math Biosci Eng, 2006. **3**(1): p. 1-15.
49. Kermack, W.O. and A.G. McKendrick, *Contributions to the mathematical theory of epidemics: IV. Analysis of experimental epidemics of the virus disease mouse ectromelia.* J Hyg (Lond), 1937. **37**(2): p. 172-87.
50. Tariq, A., et al., *Assessing reporting delays and the effective reproduction number: The Ebola epidemic in DRC, May 2018-January 2019.* Epidemics, 2019. **26**: p. 128-133.
51. *WHO. (2019). Ebola Virus Disease, Democratic Republic of Congo, External Situation Reports. April 24, 2019. Retrieved April 24, 2019. Available from:https://apps.who.int/iris/bitstream/handle/10665/312080/SITREP-EVD-DRC-20192404-eng.pdf?ua=1*.
52. Sattenspiel, L. and K. Dietz, *A structured epidemic model incorporating geographic mobility among regions.* Math Biosci, 1995. **128**(1-2): p. 71-91.
53. Merler, S., et al., *Spatiotemporal spread of the 2014 outbreak of Ebola virus disease in Liberia and the effectiveness of non-pharmaceutical interventions: a computational modelling analysis.* Lancet Infect Dis, 2015. **15**(2): p. 204-11.

Figures

Figure 1. The seven epidemiological states for individuals in the population and the transitions between states. Susceptible (S) and individuals vaccinated with either the ring or community dose of vaccine (Svr, SVc) may become exposed (E). Once exposed, individuals eventually become infectious and then refractory. Vaccinated individuals that do not become exposed eventually become immunized (M).

S	Susceptible to Ebola
Sv_c	Susceptible to Ebola but vaccinated with community dose of the vaccine
Sv_r	Susceptible to Ebola but vaccinated with ring dose of the vaccine
E	Exposed to Ebola
I	Infectious
R	Refractory after an Ebola infection
M	Immunized by the vaccine and no longer susceptible to Ebola

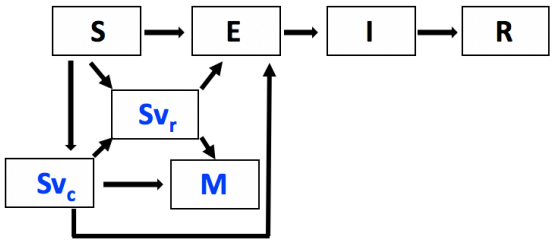

Figure 2. Description of the contact network. A) The contact network is initialized with a single infectious individual (red node) and that individual's community. For this illustrative schematic, the household size H=5 and the community size is small with C=25. The accessibility (white nodes) or inaccessibility (gray nodes) of a household is assigned randomly during the construction of the contact network. The index case happens to be in an inaccessible household: the first case of the simulation does not supply a contact list, and no contacts are vaccinated. B) After several timesteps, the infectious index case exposes another member of their household (blue node in the h_{ith} household) and a member of their community (blue node at a distance of 8 households). When the community member is exposed in the h_{i+8th} household, the total contact network is extended by 8 households to include their community (the h_{i+8th} community is outlined with a black rectangle). C) The h_{i+8th} household is accessible, so once the exposed individual becomes infectious a contact list is provided (green nodes) of households within a radius Rv=2. One household within this radius is excluded since it is inaccessible. The members of this household are not included on contact lists, do not participate in vaccination, and/or are not geographically accessible to the vaccination teams, etc.

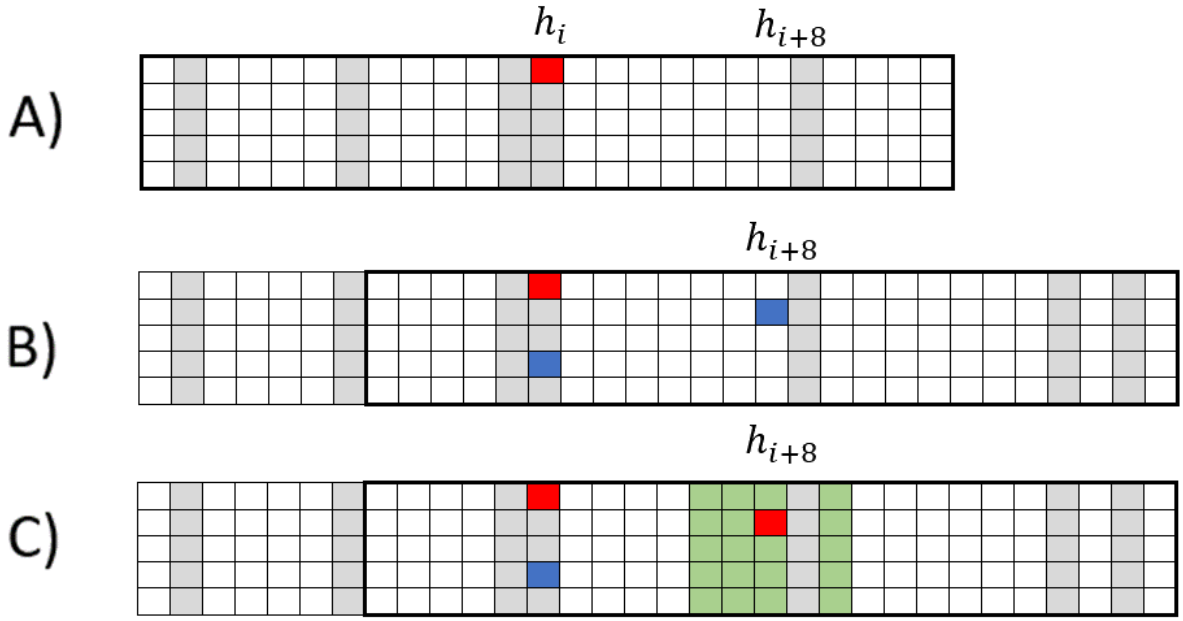

Figure 3: Community transmission profiles and steady states in the absence of vaccination. A) Transmission rates as a function of distance from an infectious individual for an inverse transmission profile (left) and exponential transmission profile (right) with community reproductive number R_{0C}=0.7 for both profiles. The inverse distance function is $g(\eta) = \frac{1}{\eta^{0.5}}$ and the exponential distance function is $f(\eta) = e^{0.13\eta}$ for the community size C=201. B). For this community size and transmission profile parameters, a steady state incidence comparable to that of the 2014-15 Ebola epidemic in Liberia is achieved when simulating epidemics in the absence of vaccination (see Figure 4).

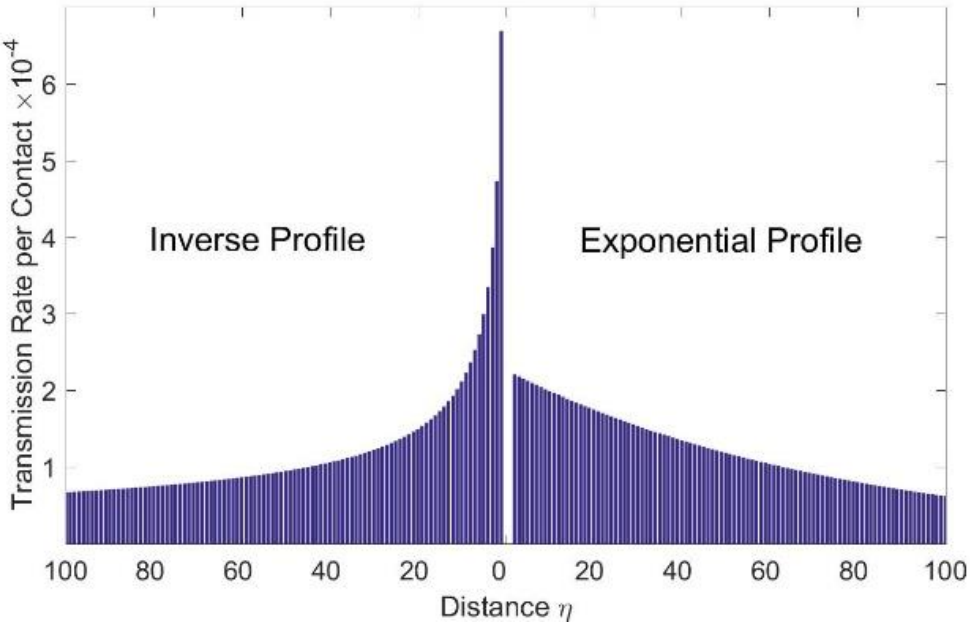

Figure 4. Probability of epidemic extinction and the baseline mean daily incidence curves in the absence of interventions for the exponential and gravity transmission profiles that define transmission rates as a function of the distance from an infectious individual (see also Figure 3). For each transmission profile, the model was calibrated by choosing the community size for each transmission profile by assuming that the ongoing Ebola outbreak in North Kivu would be similar in size to the 2014-15 Ebola outbreak in Liberia in the absence of vaccination. Outbreaks propagate through the population as spatial waves with an endemic state. The average number of cases for the n_{th} day is averaged only for the number of simulations that have not yet extinguished by day n. The error bars show the 95% confidence intervals for the mean daily incidence.

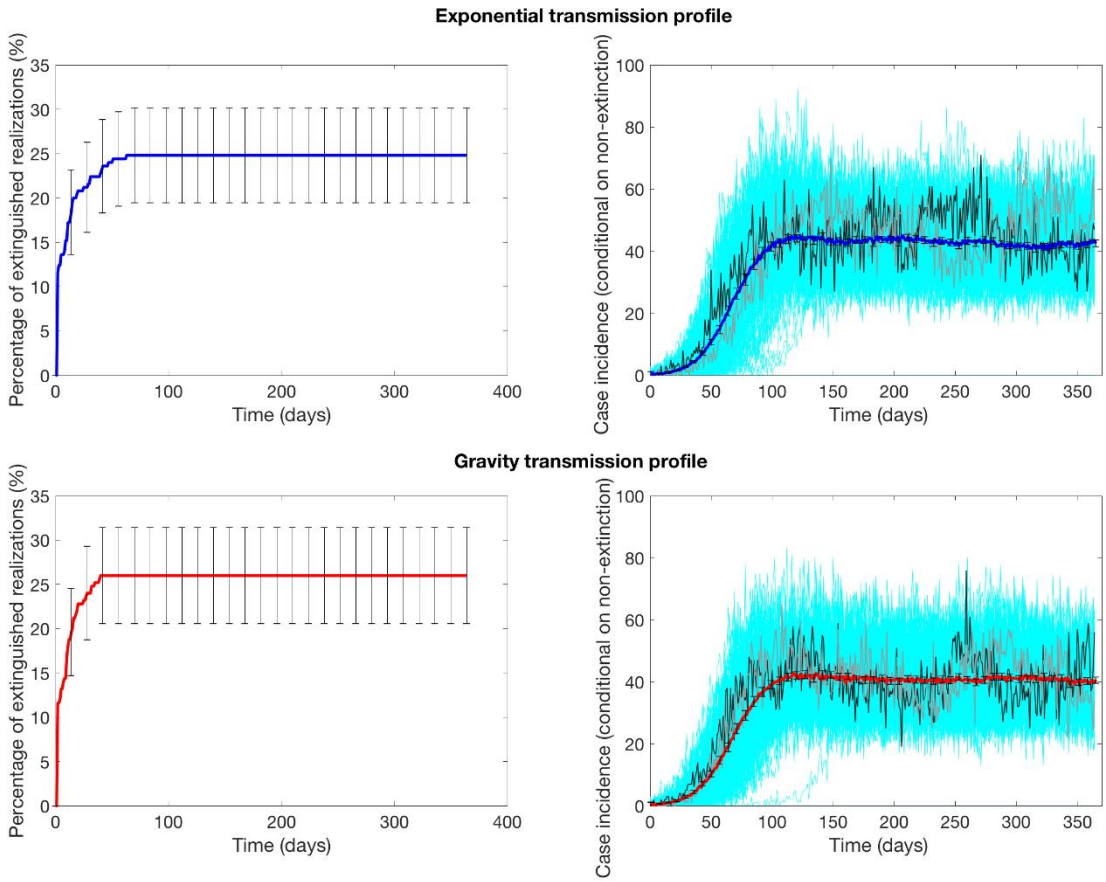

Figure 5. The impact of ring vaccination that starts 30 days after epidemic onset on the probability of outbreak extinction and the mean daily incidence curves for various percentage levels of inaccessible households, which do not participate in vaccination and do not provide contacts lists as explained in the text. These simulations were generated using the exponential transmission profile, but similar results were obtained using the gravity transmission profile described in the main text. The vertical dashed line indicates the timing of start of the ring vaccination program.

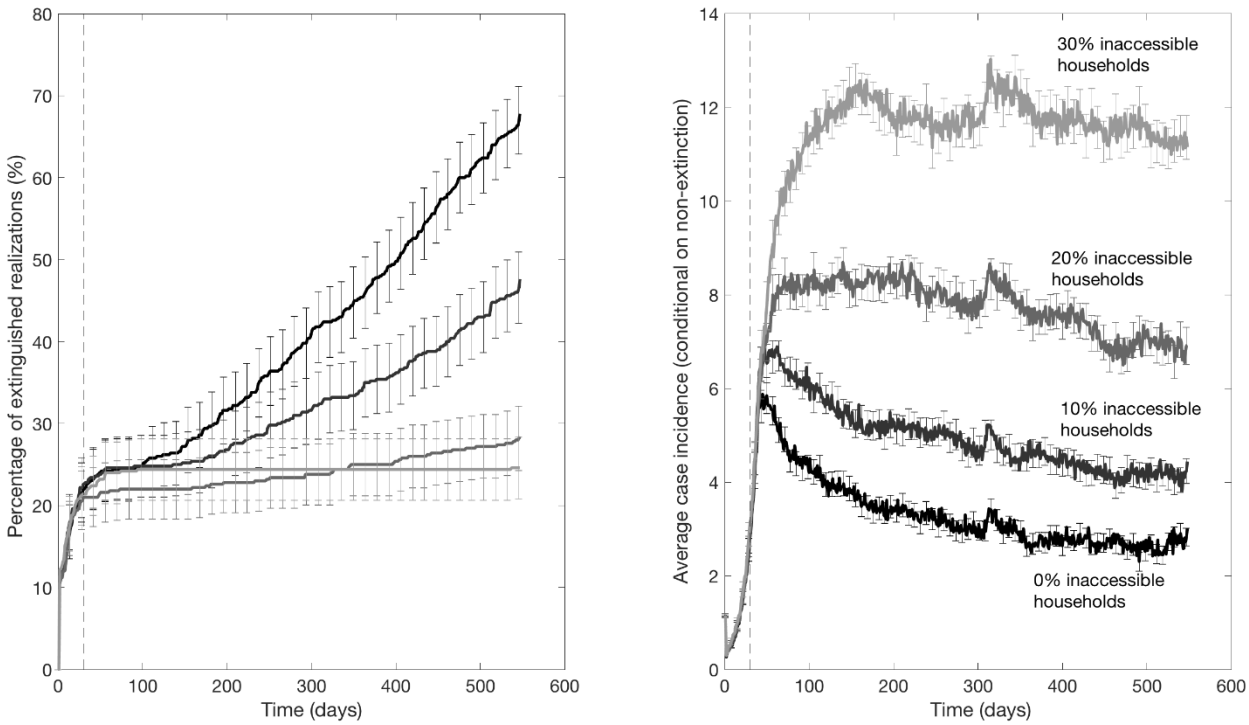

Figure 6. The impact of ring vaccination on an established epidemic wave on the probability of outbreak extinction and the mean daily incidence curves for various percentage levels of household inaccessibility. These simulations were generated using the exponential transmission profile, but similar results were obtained using the gravity transmission profile described in the main text. The vertical dashed line indicates the timing of start of the ring vaccination program. The vertical dashed line indicates that start of the ring vaccination program.

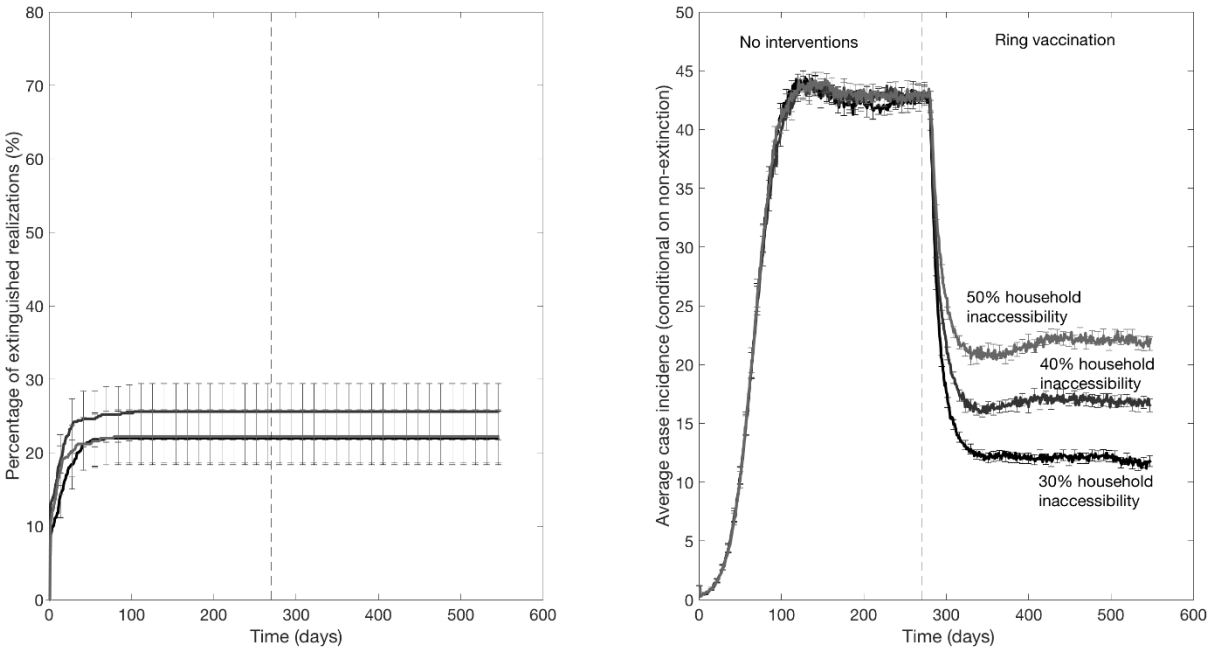

Figure 7. Mean daily case incidence when a community vaccination rate of 10% per day supplements a ring vaccination strategy 9 months later for different levels of household inaccessibility. The vertical dashed line indicates the timing of start of the supplemental community vaccination efforts. These simulations were generated using the exponential transmission profile, but similar results were obtained using the gravity transmission profile described in the main text.

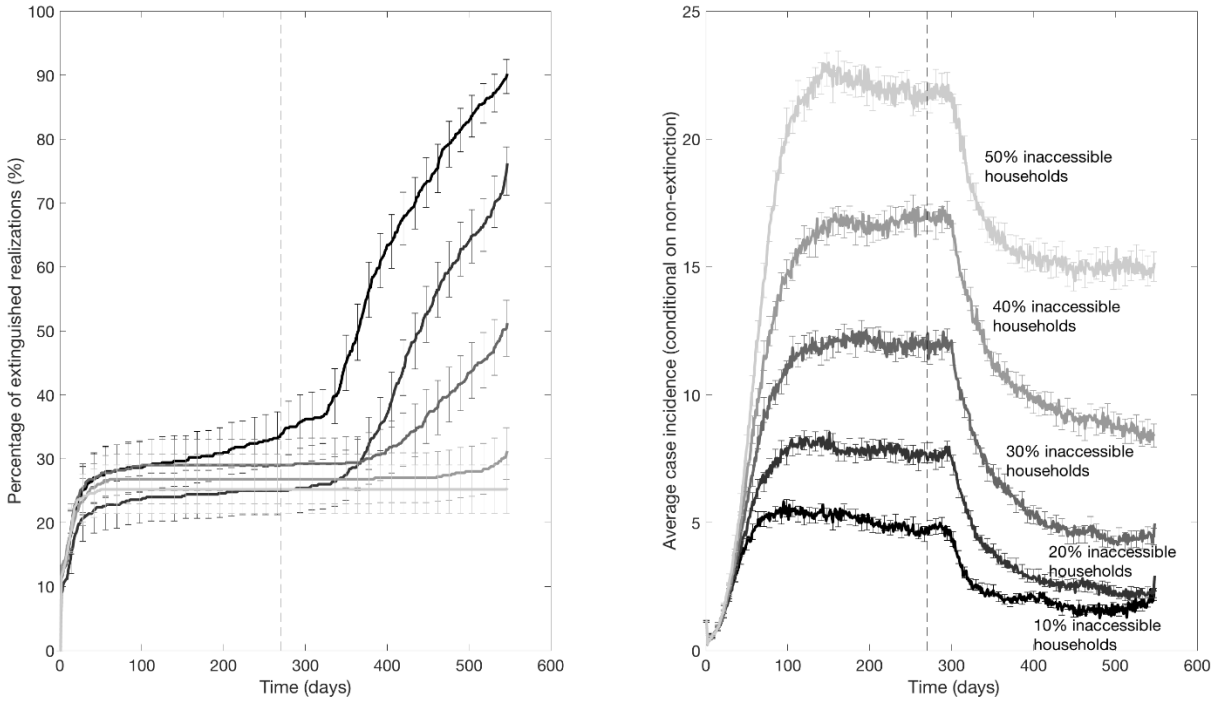

Figure 8. Probability of epidemic extinction over time and the mean daily case incidence when different community vaccination rates supplement a ring vaccination strategy for a 30% level of household inaccessibility and community vaccination starts 9 months after epidemic onset. The vertical dashed line indicates the timing of start of community vaccination. These simulations were generated using the exponential transmission profile, but similar results were obtained using the gravity transmission profile described in the main text.

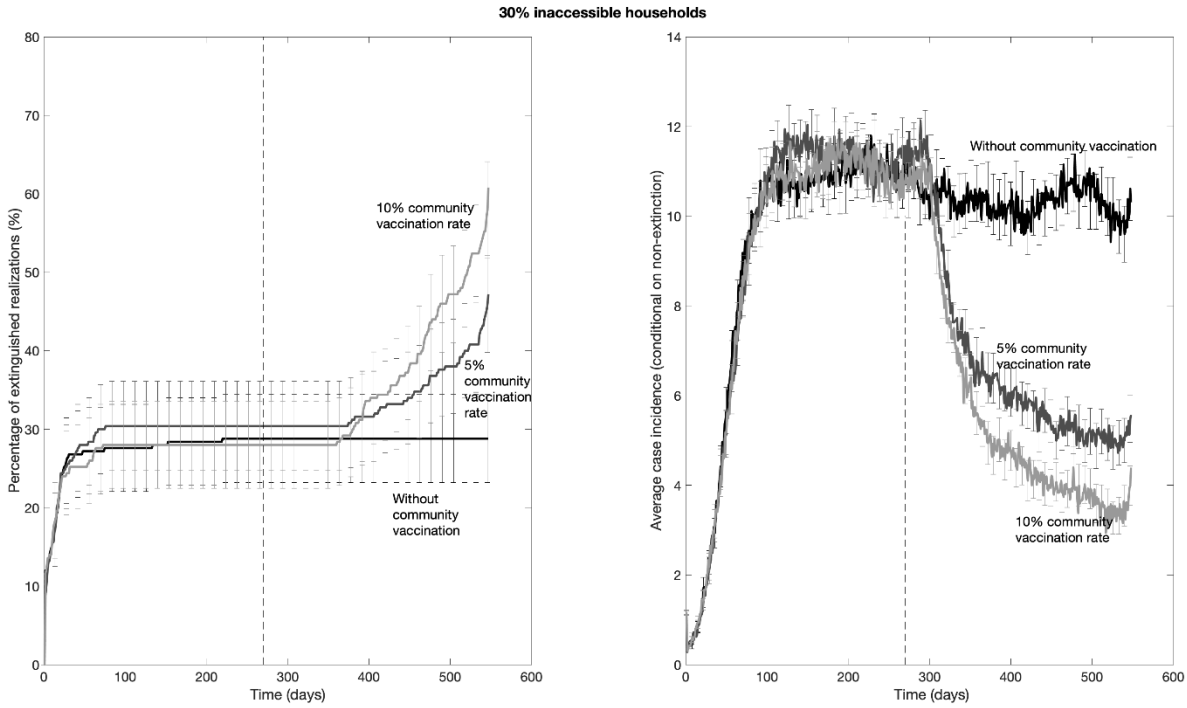
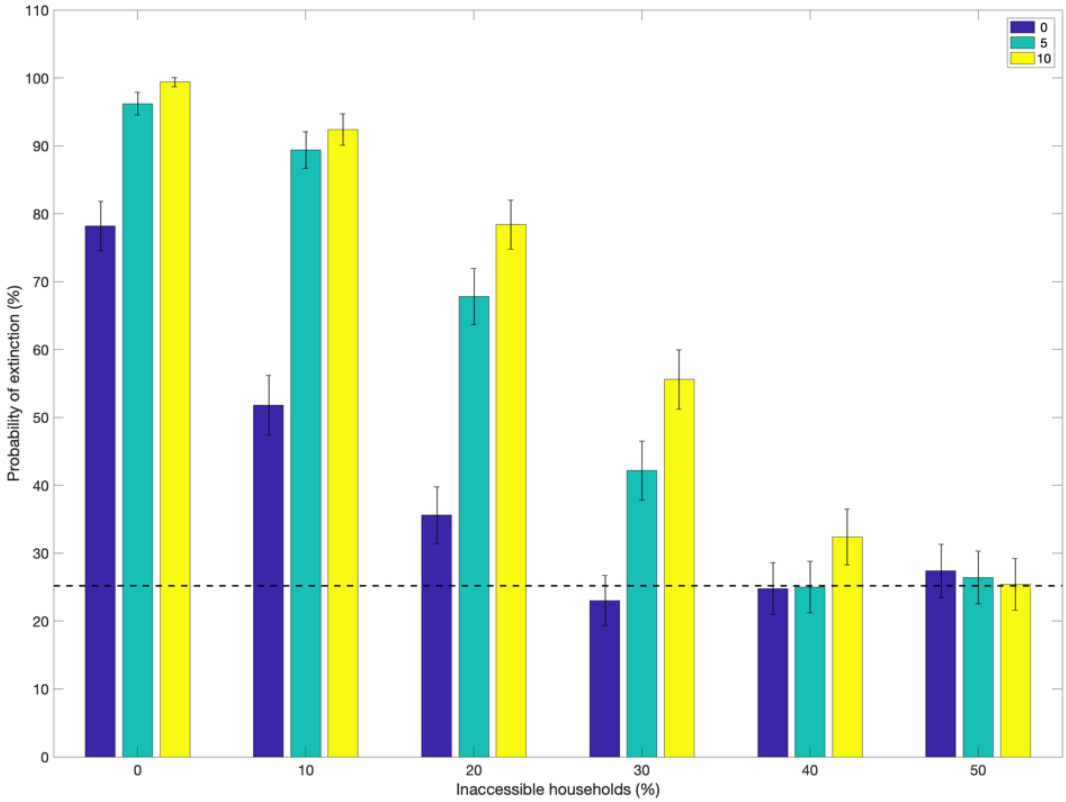
Figure 9. Supplemental effect on community vaccination on the probability of epidemic extinction for populations with different household inaccessibility levels ranging from 0 to 50%. Bars show the probability of epidemic extinction after 1.5 years for i) ring vaccination alone (blue bars), ii) community vaccination with a rate of 5% community vaccination per day (light blue bars) and iii) community vaccination with a rate of 10% vaccination per day. The horizontal line indicates the mean probability of extinction for the baseline scenario in the absence of vaccination. Timing was chosen to resemble the scenario for the DRC Ebola epidemic, with ring vaccination applied after 7 days and community vaccination applied after 9 months. These simulations were generated using the exponential transmission profile, but similar results were obtained using the gravity transmission profile described in the main text.